4-20-1997

Optical Rotation Curves of Distant Field Galaxies: Sub-L, Systems

Nicole P. Vogt
University of California, Santa Cruz

Andrew C. Phillips
University of California, Santa Cruz

S. M. Faber
University of California, Santa Cruz

Jesús Gallego
University of California, Santa Cruz

Caryl Gronwall
University of California, Santa Cruz

See next page for additional authors

THE ASTROPHYSICAL JOURNAL, 479:L121–L124, 1997 April 20

OPTICAL ROTATION CURVES OF DISTANT FIELD GALAXIES: SUB-$L^\star$ SYSTEMS[1,2]

NICOLE P. VOGT, ANDREW C. PHILLIPS, S. M. FABER, JESÚS GALLEGO,[3] CARYL GRONWALL, R. GUZMÁN, GARTH D. ILLINGWORTH, DAVID C. KOO, AND J. D. LOWENTHAL[4]
University of California Observatories/Lick Observatory, Board of Studies in Astronomy and Astrophysics, University of California, Santa Cruz, CA 95064
Received 1996 October 11; accepted 1997 February 3

ABSTRACT

Moderate-resolution spectroscopic observations from the Keck 10 m telescope are used to derive internal kinematics for eight faint disk galaxies in the fields flanking the Hubble Deep Field. The spectroscopic data are combined with high-resolution F814W Wide Field Planetary Camera 2 images from the *Hubble Space Telescope* that provide morphologies, scale lengths, inclinations, and orientations. The eight galaxies have redshifts $0.15 \lesssim z \lesssim 0.75$, magnitudes $18.6 \leq I_{814} \leq 22.1$, and luminosities $-21.8 \leq M_B \leq -19.0$ ($H_0 = 75$ km s^{-1} Mpc^{-1} and $q_0 = 0.05$). Terminal disk velocities are derived from the spatially resolved velocity profiles by modeling the effects of seeing, slit width, slit misalignment with galaxy major axis, and inclination for each source. These data are combined with the sample of Vogt et al. to provide a high-redshift Tully-Fisher relation that spans 3 magnitudes. This sample was selected primarily by morphology and magnitude, rather than color or spectral features. We find no obvious change in the shape or slope of the relation with respect to the local Tully-Fisher relation. The small offset of $\lesssim$0.4 mag in B with respect to the local relation is presumably caused by luminosity evolution in the field galaxy population and does not correlate with galaxy mass. A comparison of disk surface brightness between local and high-redshift samples yields a similar offset, $\sim$0.6 mag. These results provide further evidence for only a *modest* increase in luminosity with look-back time.

Subject headings: galaxies: evolution — galaxies: kinematics and dynamics

1. INTRODUCTION

Until recently, studies of faint field galaxies have been limited to galaxy counts, colors, and redshift distributions, which can be used to construct luminosity functions at earlier epochs. Such luminosity functions are then compared with models incorporating a certain amount of number evolution (controlled by galaxy formation and merging) coupled with luminosity and color evolution (controlled by star formation histories). Recent models range from those predicting only a small degree of luminosity evolution (e.g., Gronwall & Koo 1995) to those invoking entirely new classes of galaxies (e.g., Babul & Rees 1992; Babul & Ferguson 1996) to those requiring high merger rates (e.g., Broadhurst, Ellis, & Glazebrook 1992). A direct measure of luminosity evolution in field galaxies will help to distinguish between various hypotheses. Such measures have been attempted recently, but the results are somewhat contradictory. Schade et al. (1996a) found evidence for disk brightening by 1.2 mag in B in galaxies at redshifts $0.5 \leq z \leq 1.2$. Simard & Pritchet (1997) found even greater levels of evolution (2.5 ± 0.5 mag) in a sample of very blue galaxies at $z \sim 0.35$ for which strong [O II] lines could be spatially resolved. Rix et al. (1997), also using kinematic information, derived a brightening of 1.5 mag at $z \sim 0.25$ for sub-$L^\star$ galaxies. In contrast, Vogt et al. (1996) and Bershady (1997), using optical rotation curves, and Forbes et al. (1996), using line widths, found only small deviations from the local Tully-Fisher (TF) relation (Tully & Fisher 1977) for spiral galaxies, implying only modest brightening ($\sim$0.4 mag) out to $z \sim 1$. Simard & Pritchet postulate that these various results could be reconciled if strong luminosity evolution were present *only* in lower mass systems. If confirmed, this would be an important factor in understanding the evolution of field galaxies.

This Letter introduces well-resolved rotation curves of eight predominantly lower luminosity galaxies ($L_B \lesssim L_B^\star = -20.3$; see Efstathiou, Ellis, & Peterson 1988), selected by morphology as suitable TF candidates. These new observations provide a valuable test of the mass-dependent luminosity evolution hypothesis, particularly in comparison with the higher mass sample presented by Vogt et al. (1996, hereafter Paper I). Combined with the work of Paper I, these data form a sample of rotation curves for 16 galaxies at redshifts $0.15 \lesssim z \lesssim 1$, ranging over half the age of the universe (for $q_0 = 0$, one-third for $q_0 = 0.5$). We also use this combined data set to explore trends in surface brightness for comparison with Colless et al. (1994), Forbes et al. (1996), and Schade et al. (1996a). Detailed analysis of a significantly larger data set is currently underway, and these results will be used to explore a variety of relevant selection effects. A full description of our analysis techniques is deferred to that paper (Vogt et al. 1997).

2. OBSERVATIONS

The TF candidate objects were selected from the Wide Field Planetary Camera 2 (WFPC2) F814W (I_{814}) images of the flanking fields of the Hubble Deep Field (HDF; Williams et al. 1996). Selection was based on the following criteria: (i) undistorted disk morphology; (ii) inclination greater than 30°; (iii) no interacting companions or obscuring foreground stars;

[1] Based on observations obtained at the W. M. Keck Observatory, which is operated jointly by the California Institute of Technology and the University of California.

[2] Based in part on observations with the NASA/ESA *Hubble Space Telescope*, obtained at the Space Telescope Science Institute, which is operated by AURA, Inc., under NASA contract NAS 5-26555.

[3] Current address: Dept. Astrofísica, Universidad Complutense, E-28040 Madrid, Spain.

[4] Hubble Fellow.

and (iv) $I_{814} \leq 22.5$. The selection was made with no a priori knowledge of redshifts or luminosities. The galaxies were observed in 1996 April under the auspices of the Deep Extragalactic Evolutionary Probe (DEEP) project (Koo 1995), using the Low-Resolution Imaging Spectrograph (LRIS; Oke et al. 1995) on the Keck 10 m telescope. LRIS employs slit masks to provide "long-slit" spectral observations for multiple objects simultaneously. For the TF candidates, the slitlet for each object was tilted to align with the major axis of each galaxy. Slitlets were 1".1 wide and $\geq$12".0 long for these objects. Integration times were 50 minutes for each of two 600 line mm^{-1} gratings, blazed at 5000 and 7500 Å; the combined spectral range was roughly 3800–8600 Å. Spectral and spatial scales were 1.28 Å $pixel^{-1}$ and 0".215 $pixel^{-1}$, respectively. The seeing was approximately 1".0 FWHM. In addition to spectroscopy, two 300 s V-band images of the field were acquired (see Phillips et al. 1997 for more details of the observations and for galaxy coordinates).

The new spectral data have several significant improvements over those of Paper I. The targets were preselected as suitable TF galaxies, whereas the rotation curves in Paper I were obtained serendipitously. Slitlets were aligned with the galaxy major axes, removing a source of potentially significant error. Finally, the expanded spectral range means that multiple emission lines were observed for each object, e.g., [O II] λ3727 through [O III] λ5007 for $z < 0.7$ (the majority of our sources), and through Hα for $z < 0.3$. For $z > 0.7$, only the [O II] lines were available.

3. DATA REDUCTION AND ANALYSIS

3.1. *Spectral Measurements*

The LRIS spectra were debiased and flat-fielded, and then rectified. Wavelength calibration was done using the procedure described in Kelson et al. (1997). No relative or absolute flux calibration was applied. All spectra (not just those preselected for TF work) were examined for spatially extended emission lines, but only one additional object (IE 4-1304-1007) displayed such lines (the apparent inclination of this object was too low for our criteria, but we include it in our final sample). Among the 18 preselected candidates, one has yielded no redshift identification; one has a pure early-type spectrum with no detected emission lines; one at $z = 0.109$ displayed unusually weak lines, both in emission and absorption; eight show normal disk galaxy spectra, but the emission lines are too weak to use to derive velocity curves; and seven display emission lines of sufficient strength to determine velocity structure. The group of eight has virtually the same median redshift (0.50) and redshift range (0.41–0.77) as do the seven successful targets.

The [OII] λ3727 doublet, Hβ, and [O III] λ5007 were observed for most sources in the final sample. The spatially resolved emission lines were analyzed using the same Gaussian profile fitting technique described in Paper I (see also Vogt 1995). Briefly, a single (or double) Gaussian profile was used to fit each emission line (or doublet) at each point in the spatial direction. Profiles were considered acceptable whenever the Gaussian fit met minimum requirements in height and width, generally a signal-to-noise ratio (S/N) of 5 σ and 3 σ, respectively; the typical value was 10 σ for both width and amplitude. Central wavelengths of the profiles were used to construct observed rotation curves.

As discussed in Paper I, the sizes of the disks in these galaxies are on the order of the seeing and the slit width. Thus, wavelength shifts in the observed spectral lines are not only a function of the velocity profile of the disk, but also the surface brightness distribution and the mapping of the seeing-smoothed flux through the full slit. (A simplifying factor for the new data is that the misalignment of the slit relative to the galaxy major axis was less than 10° for all but one source.) To derive terminal velocities, we must correct for these effects. To this end, we employ a grid of simple exponential disk models with different terminal velocities in order to simulate emission lines, and we fit these model emission lines identically to the spectral data. The circular velocity of the galaxy model was adjusted iteratively to match the observed data and was adopted as the intrinsic terminal velocity, $V_{\rm term}$. (For some galaxies, a clear turnover in the velocity curve was not observed. Rather than match the inner, rising rotation curve and extrapolate to a turnover velocity, we have chosen the model whose measured turnover velocity matches the maximum velocity measured in our spectra; these models provide lower limits to the true $V_{\rm term}$.) Errors in $V_{\rm term}$ were estimated by varying the inclination and position angle of each galaxy by $\pm$10°.

3.2. *Photometric Parameters*

The *Hubble Space Telescope* (*HST*) I_{814} images were analyzed using IRAF-based tools (see, e.g., Forbes et al. 1994; Phillips et al. 1997). Total magnitudes were measured from aperture growth curves; inclinations and position angles were estimated from outer elliptical isophotes; and disk scale lengths were measured from simultaneous disk-plus-bulge fits to the major-axis intensity profiles. *HST* took images of the flanking fields in I_{814} only, so a LRIS V image was used to determine a $V - I$ color. The I_{814} image was seeing-degraded to match the ground-based image, and the color was determined within a 2".2 diameter aperture (see Phillips et al. 1997 for more detail).

Intrinsic galaxy parameters were calculated using the measured redshifts, photometry, and angular scales, assuming $H_0 = 75$ km s^{-1} Mpc^{-1} and $q_0 = 0.05$.[5] To determine rest-frame luminosities, L_B, k-corrections were interpolated from the model spectral energy distributions (SEDs) of Gronwall & Koo (1995), which are based on Bruzual & Charlot (1993) models and realistic star formation scenarios. Current epoch (i.e., nonevolving) SEDs were used. Since rest-frame B corresponds to observed V_{606} at $z \sim 0.4$ and to I_{814} at $z \sim 0.8$, errors in the k-corrections should be small. Galactic extinction was taken to be negligible for the HDF (Williams et al. 1996), and sources were corrected for internal extinction following the method of Tully & Fouqué (1985) in order to be consistent with Pierce & Tully (1988, 1992).

4. RESULTS AND DISCUSSION

Images of the eight new galaxies and their spatially resolved [O II] lines are shown in Figures 1*a* and 1*b* (Plates L8 and L9), along with the observed and modeled velocity curves. Like the eight galaxies discussed in Paper I, these new distant TF galaxies appear to be quite similar to local normal spiral galaxies, both morphologically and kinematically. The *HST* images show apparently normal, disk-dominated spirals. Allowing for seeing and resolution effects, the velocity curves are qualitatively similar to those of local spirals. The rotation curves are traceable to ~3 exponential scale lengths (R_d) in the disks, a length comparable to the extent of rotation curves for local galaxies (cf. Vogt 1995). A simple estimate of their

[5] The data from Paper I have been adjusted for these new values.

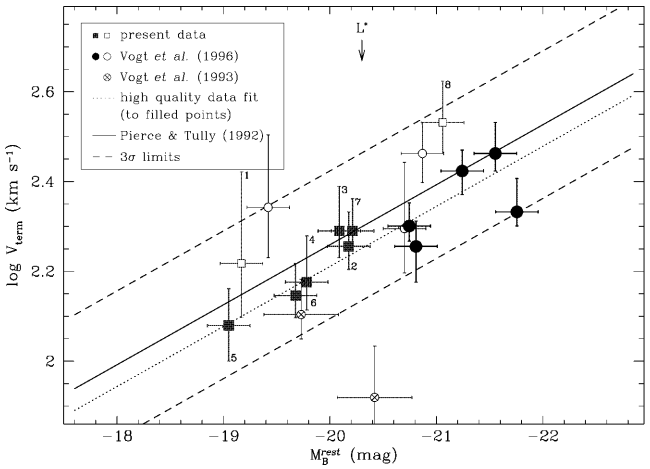

FIG. 2.—A high-redshift TF diagram plotting $V_{\rm term}$ vs. B luminosity. We show our data (numbered in increasing redshift) and those from Vogt et al. (1993) and Paper I compared with the relationship (*solid line*) based on H I velocity width measurements of a restricted set of 32 local cluster spirals (Pierce & Tully 1992). The dashed lines are the 3 σ limits to the dispersion in this local relation. Velocities have been corrected by sin i, and the magnitudes corrected for internal extinction. We adopt $H_0 = 75$ km s^{-1} Mpc^{-1} and $q_0 = 0.05$. Assuming the same slope as that of the local sample, the weighted fit (*dotted line*) to our 11 high-quality points (*filled symbols*) is offset from the local relation by 0.36 ± 0.13 mag toward higher luminosity.

masses, $M = V^2R/G$, yields values of (0.5–5) $\times$ 10^{11} $M_\odot$ within 15 kpc, similar to the range of masses found for nearby spirals.

For purposes of discussion, we separate the velocity data into two classes. High quality is defined as having sufficient S/N and resolution elements to clearly determine a terminal velocity, at least one emission line free of strong night-sky contamination, apparent inclination greater than 30°, and a slit misaligned with the galaxy major axis by less than 20°. Six of the eight new galaxies and five from Paper I meet these criteria. Note that the serendipitous object, IE 4-1304-1007, is a low-quality source.

4.1. *TF Relation at High-Redshift*

In Figure 2, we compare the 16 galaxies with a local TF relation in the rest-frame B band. The local relation shown is an *inverse* fit (i.e., $V_{\rm term}$ as a function of M_B) to the local sample from Pierce & Tully (1992); this is the proper fit for comparison with a magnitude-limited sample (see Paper I). The 11 high-quality sources have a weighted offset of 0.36 ± 0.13 mag relative to the local relation and an rms dispersion of 0.65 mag. This observed dispersion matches the combined estimated errors of the logarithmic velocity widths (0.47), the rest-frame B magnitudes (0.2), and an assumed intrinsic scatter in the TF relation (0.4; cf. Willick et al. 1996 and references therein), thus helping to validate our error estimates. The lower quality points show a much larger scatter, as expected.

We emphasize that the derived offset, $\sim$0.4 mag, represents an *upper limit* to luminosity evolution of field galaxies, for these reasons: any magnitude-limited sample is biased toward more luminous objects; our analysis is restricted to objects with detectable emission lines—that is, actively star-forming galaxies that are likely to have elevated B luminosities; some terminal velocities are lower limits; and we may be overcorrecting for extinction if galaxies were less dusty at earlier epochs. Our choice of $q_0 = 0.05$ is also conservative—derived luminosities are reduced by 0.1–0.4 mag for $q_0 = 0.5$. While mass evolution is a possible factor, we have assumed implicitly that evolution in luminosity dominates the observed offset. We do not expect the masses to evolve strongly, though, given the presence of clearly formed disks.

The new HDF data extend the luminosity range of our total sample to $-21.8 \lesssim M_B \lesssim -19$. It is notable that *there is no deviation from a linear relation over this range*, i.e., there is no evidence in these data for different amounts of luminosity evolution in different luminosity or mass regimes.

One explanation for the wide range in luminosity evolution found by various groups is that sample selection strongly affects the degree of evolution detected in a given sample. In our sample, the galaxies were chosen primarily by morphology. On the other hand, Bershady (1997), Simard & Pritchet (1997), and Rix et al. (1997) selected *blue* galaxies. These studies all had different sample selection, redshift ranges, and observational and analysis techniques; a direct comparison is not practical nor is a full discussion of these parameters within the scope of this Letter (see Vogt et al. 1997). However, it is useful to consider the potentially critical issue of color-selection criteria. The Bershady (1997) low-redshift ($0.05 \leq z \leq 0.35$) sample shows an offset of less than 0.5 mag, while the Rix et al. (1997) spatially unresolved data at redshift $z \sim 0.25$ show evidence for a magnitude offset of $\sim$1.5 relative to a local *blue* sample (i.e., the effect would be even greater if the data were compared with a general local sample). Simard & Pritchet (1997) chose the strongest [O II] emitters from among a sample of emission-line galaxies (Simard 1996), and they found the highest offset of all (2.5 ± 0.5 mag for a redshift of $z \sim 0.35$; note the large scatter). This suggests that the bluest, most actively star-forming galaxies may show the largest offsets. Forbes et al. (1996), whose sample was not color-selected, noted some correlation between their offsets and their galaxy colors in the sense that the galaxies with the largest offsets tended to be blue. Rix et al. (1997) find the same trend within their blue sample. As a further example, Figure 2 includes the two galaxies from Vogt et al. (1993) with observed optical rotation curves; one (SA 68-2545.3) was chosen specifically for its unusually strong [O II] flux, and this galaxy shows a very large offset from the TF relation. Taken together, this suggests that for redshifts $z \gtrsim 0.2$, color may prove to be a good indicator of luminosity evolution in field galaxies, distinguishing between an average, stable population and a bluer, star-forming population with enhanced luminosity.

4.2. *Surface Brightness Evolution*

Changes in surface brightness levels in disk galaxies can provide an independent determination of luminosity evolution, provided scale lengths do not evolve strongly, and is particularly useful since it is independent of q_0. Freeman (1970) showed that disks in local spiral galaxies have a near-uniform central surface brightness ($\mu_B = 21.65$ mag arcsec^{-2}). Recently, de Jong (1995) found a morphological-type dependence to the surface brightness and studied the effect of internal extinction, determining a value of $\mu_B = 21.45 \pm 0.76$ mag arcsec^{-2} for the case of spirals with T-types 1–6 (de Vaucouleurs et al. 1991) with semitransparent disks. Among high-redshift ($z \sim 0.5$) galaxies, Forbes et al. (1996) concluded that the surface brightness increases by 0.6 ± 0.1 mag with respect to local galaxies of similar mass. This is also in agreement with Colless et al. (1994). Schade et al. (1996a, 1996b) find increases of $\sim$0.9 mag out to a redshift $z \sim 0.5$ and

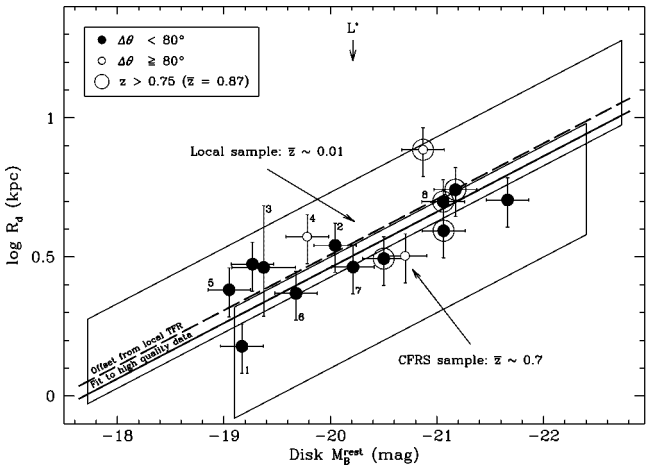

FIG. 3.—Disk surface brightness evolution diagram. Exponential disk scale lengths, R_d (uncorrected for inclination), are plotted vs. disk B luminosity for the 15 disk galaxies in our sample (new sources are numbered in increasing redshift as in Fig. 2). The five sources with redshift $0.75 \leq z \leq 1$ are circled. Open symbols denote disks with apparent inclination $i \geq 80°$, which may suffer from large systematic errors (see text). Note that R_d was measured from the major-axis profile, with a disk and $r^{1/4}$-law bulge fitted simultaneously. The median B/D ratio is 0.1; this value is generally consistent with the Forbes et al. (1996) and Colless et al. (1994) sample of faint field galaxies. The region occupied by local spirals (from de Jong 1995) is lightly shaded; the region populated by the galaxies at redshift $\bar{z} \sim 0.7$ from Schade et al. (1996a) is darker (arrows point to median values). The solid line is the offset (0.59 ± 0.13 mag) found by a weighted fit to the 12 disks with inclination angles less than 80°, while the dashed line indicates the luminosity offset (0.36 ± 0.13 mag) found with respect to the local TF relation (Fig. 2).

1.6 ± 0.1 mag for disk galaxies at redshifts $0.5 < z < 1.1$, respectively (with no correction for internal extinction). For our sample, we compare disk sizes and luminosities for the 15 disk galaxies, as plotted in Figure 3 (we exclude the "double nucleus" galaxy from Paper I, since its structure is complex). The single early-type spiral (NE 4-1269-1248) appears to be a "ring galaxy" whose profile is difficult to fit. Scale length measurements for it range from 0.″4 to 1.″0; we adopt 0.″6 (with large uncertainties) since it appears most credible. This galaxy also has a significantly larger bulge-to-disk (B/D) ratio (~0.9) than that of the others (~0.1). As is normal practice, the disk scale lengths have not been corrected to face-on values. Sources with inclination $i \gtrsim 80°$ may be systematically in error, because of distortion of the surface brightness profiles from nonuniform extinction at different radii (cf. Giovanelli et al. 1994). A comparison is made with de Jong's local galaxy sample and distant galaxy measurements from Schade et al. (1996a). We find our sample to have an overall offset of 0.59 ± 0.13 mag with respect to local galaxies, in fairly good agreement with the offset in the TF relation. Although the highest redshift data ($z > 0.75$) generally lie within the locus of the data points from Schade et al., the median offset in our data is significantly less. The apparent brightening at the high-mass end (seen also in the data of Forbes et al. 1996) could be caused by a bias toward higher than average luminosities among the most distant objects, as well as by luminosity evolution.

5. CONCLUSIONS

In summary, we have compared a set of 16 high-redshift galaxies with a local TF relation and find a modest amount of luminosity evolution ($\Delta M_B \lesssim 0.4$). This conclusion is supported by an examination of the surface brightness characteristics of the sample, which show evidence for evolution at the level of ~0.6 mag. We find no evidence for deviation from a linear TF relation at lower luminosities to a magnitude $M_B \sim -19$. The bluest galaxies within the sample have a slightly larger offset from the local TF relation, which suggests (when taken in conjunction with results of other studies) that the derived degree of luminosity evolution may depend strongly on sample selection.

DEEP was established through the Center for Particle Astrophysics. Funding was provided by NSF grants AST-9529098, AST-922540, and AST-9120005 and NASA grants AR-06337.08-94A, AR-06337.21-94A, GO-05994.01-94A, AR-5801.01-94A, and AR-6402.01-95A. J. G. acknowledges partial support from Spanish MEC grants PB89-124 and PB93-456, and a UCM del Amo foundation fellowship; C. G. acknowledges funding from an NSF Graduate Fellowship; and J. D. L. acknowledges support from NASA grant HF-1048.01-93A.

REFERENCES

Babul, A., & Ferguson, H. C. 1996, ApJ, 458, 100
Babul, A., & Rees, M. 1992, MNRAS, 255, 346
Bershady, M. A. 1997, in ASP Conf. Ser., Dark and Visible Matter in Galaxies and Cosmological Implications, ed. M. Persic & P. Salucci (San Francisco: ASP), in press
Broadhurst, T. J., Ellis, R. S., & Glazebrook, K. 1992, Nature, 355, 55
Bruzual, A. G., & Charlot, S. 1993, ApJ, 405, 538
Colless, M., Schade, D., Broadhurst, T. J., & Ellis, R. S. 1994, MNRAS, 267, 1108
de Jong, R. S. 1995, Ph.D. thesis, Univ. Groningen
de Vaucouleurs, G., de Vaucouleurs, A., Corwin, H. G., Buta, R. J., Paturel, G., & Fouqué, P. 1991, Third Reference Catalogue of Bright Galaxies (New York: Springer)
Efstathiou, G., Ellis, R. S., & Peterson, B. A. 1988, MNRAS, 232, 431
Forbes, D. A., Elson, R. A. W., Phillips, A. C., Illingworth, G. D., & Koo, D. C. 1994, ApJ, 437, L17
Forbes, D. A., Phillips, A. C., Koo, D. C., & Illingworth, G. D. 1996, ApJ, 462, 89
Freeman, K. C. 1970, ApJ, 160, 811
Giovanelli, R., Haynes, M. P., Salzer, J. J., Wegner, G., da Costa, L. N., & Freudling, W. 1994, AJ, 107, 2036
Gronwall, C., & Koo, D. C. 1995, ApJ, 440, L1
Kelson, D. D., van Dokkum, P., Franx, M., & Illingworth, G. D. 1997, ApJ, 478, 430
Koo, D. C. 1995, in Wide Field Spectroscopy and the Distant Universe, ed. S. Maddox & A. Aragón-Salamanca (Singapore: World Scientific), 55
Oke, J. B., et al. 1995, PASP, 107, 375
Phillips, A. C., et al. 1997, in preparation
Pierce, M. J., & Tully, R. B. 1988, ApJ, 330, 579
———. 1992, ApJ, 387, 47
Rix, H.-W., Guhathakurta, P., Colless, M., & Ing, K. 1997, MNRAS, in press
Schade, D., Carlberg, R. G., Yee, H. K. C., López-Cruz, O., & Ellingson, E. 1996a, ApJ, 465, L103
Schade, D., Lilly, S. J., Le Fèvre, O., Hammer, F., & Crampton, D. 1996b, ApJ, 464, 79
Simard, L. 1996, Ph.D. thesis, Univ. Victoria
Simard, L., & Pritchet, C. 1997, ApJ, submitted
Tully, R. B., & Fisher, J. R. 1977, A&A, 54, 661
Tully, R. B., & Fouqué, P. 1985, ApJS, 58, 67
Vogt, N. P. 1995, Ph.D. thesis, Cornell Univ.
Vogt, N. P., Forbes, D. A., Phillips, A. C., Gronwall, C., Faber, S. M., Illingworth, G. D., & Koo, D. C. 1996, ApJ, 465, L15 (Paper I)
Vogt, N. P., Herter, T., Haynes, M. P., & Courteau, S. 1993, ApJ, 415, L95
Vogt, N. P., et al. 1997, in preparation
Williams, R. E., et al. 1996, AJ, 112, 1335
Willick, J. A., Courteau, S., Faber, S. M., Burstein, D., Dekel, A., & Kolatt, T. 1996, ApJ, 457, 460

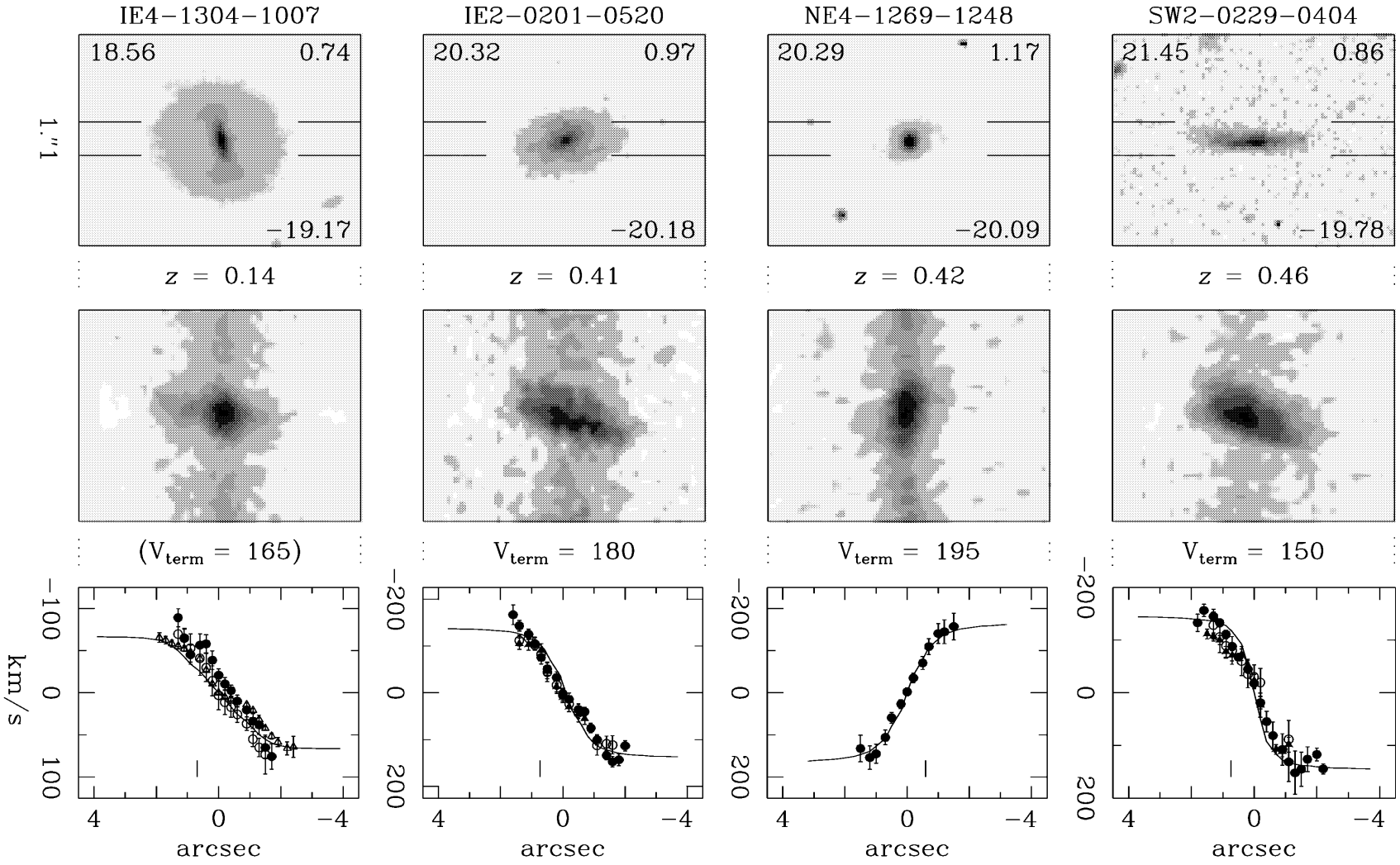

FIG. 1*a*

FIG. 1.—HDF galaxies and their velocity curves. Scales are identical, and spatial axes are aligned for each set of three plots. *Top panels*: the WFPC2 *I*-band image of each galaxy, along with its I_{814}, V_{606}–I_{814}, and M_B magnitudes and the LRIS slit width and orientation. *Middle panels*: a ~40 Å section of the LRIS spectrum centered around the redshifted [O II] λ3727 doublet. In the velocity plots (*bottom panels*), points represent the observed velocities: (*filled circle*) [O II], (*filled triangle*) Hβ, (*open circle*) [O III] λ5007, and (*open triangle*) Hα. Error bars are internal errors from the line-fitting technique. Data are shown only where the S/N was adequate; the Hβ and [O III] lines are not fitted for several sources because of weak line strength, interference caused by night-sky OH emission lines, or fringing in the red portion of the spectrum. The solid line is the fit to the model emission line(s), and the intrinsic circular velocity of the model is noted (parentheses indicate lower quality sources). A small tick marks the measured disk scale length. IE 4-1304-1007: all emission lines plus [N II] λ6583 were traced (only three are shown for legibility), but the strong bar and face-on nature of this galaxy make this a poor candidate. IE 2-0201-0520: measured [O II] velocities are somewhat larger than [O III] and Hβ, so the median velocity at each radius was fitted. NE 4-1269-1248: early-type ring galaxy with [O II] flux concentrated in core; [O III] and Hβ is too weak to trace. OE 4-0981-1325: [O III]; Hβ is too weak to trace. SE 2-0304-0307: note good agreement between [O II] and both [O III] and Hβ, observed with different gratings. NW 2-0358-0561: note excellent agreement of Hβ and [O II]. IE 2-0229-0212: night-sky line bisects [O II] emission, leading to large uncertainties.

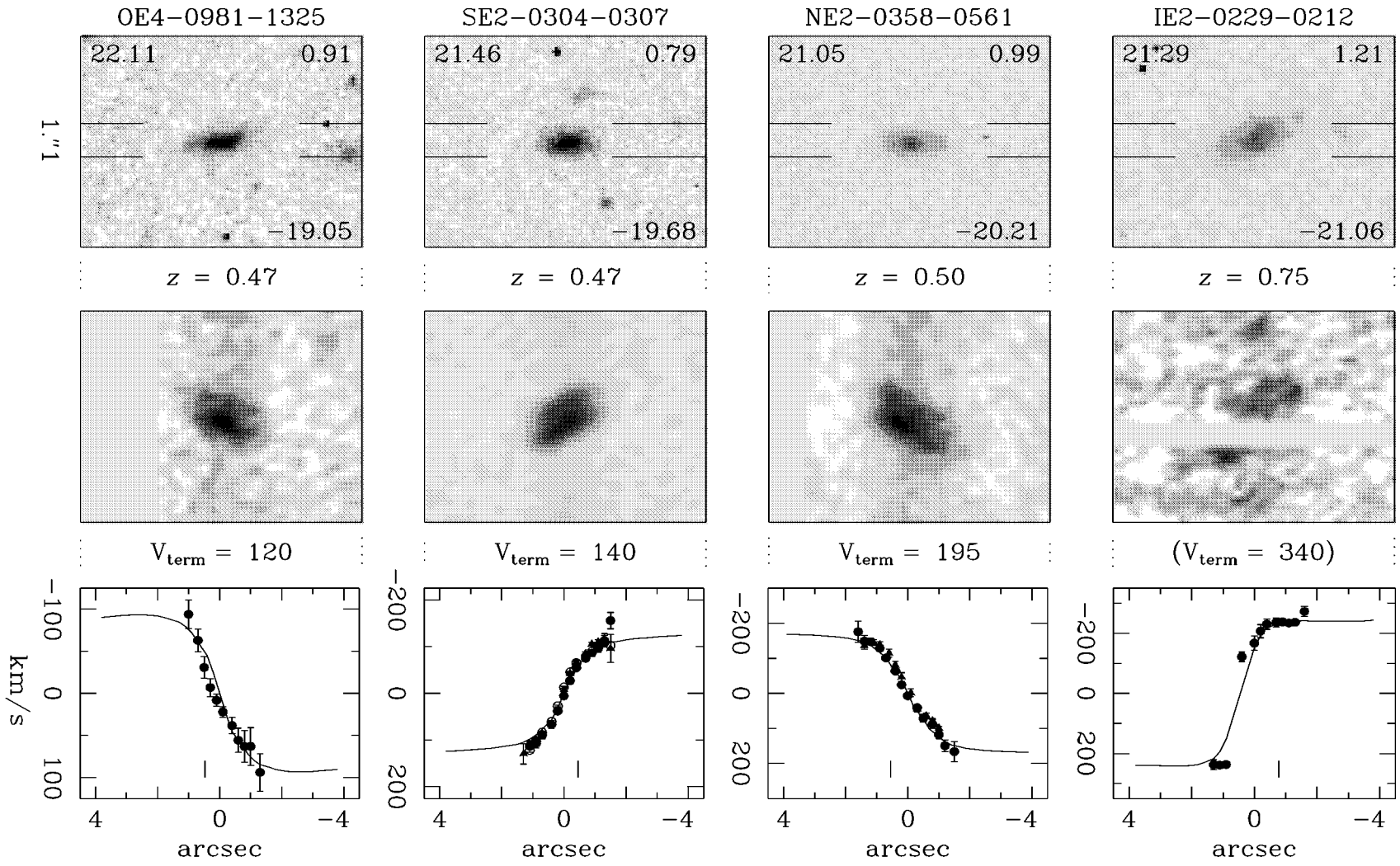
OE4−0981−1325
SE2−0304−0307
NE2−0358−0561
IE2−0229−0212
22.11
0.91
−19.05
21.46
0.79
−19.68
21.05
0.99
−20.21
21.29
1.21
−21.06
1."1
z = 0.47
z = 0.47
z = 0.50
z = 0.75
V_term = 120
V_term = 140
V_term = 195
(V_term = 340)
km/s
−100
0
100
−200
0
200
−200
0
200
−200
0
200
4
0
−4
arcsec

FIG. 1*b*